The authors wish to thank Dr A. C. Willis for generous assistance with X-ray data collection.

References

ALCOCK, N. W. (1970). *Acta Cryst.* A**26**, 437–439.

BROWN, I. D. (1978). *Chem. Soc. Rev.* **7**, 359–376.

BROWN, I. D. (1981). *Structure and Bonding in Crystals*, Vol. 2, edited by M. O'KEEFFE & A. NAVROTSKY, pp. 1–30. New York: Academic Press.

BROWN, I. D. & ALTERMATT, D. (1985). *Acta Cryst.* B**41**, 244–247.

COPPENS, P. & HAMILTON, W. C. (1970). *Acta Cryst.* A**26**, 71–83.

DORRIAN, J. F., NEWNHAM, R. E., SMITH, T. K. & KAY, M. I. (1971). *Ferroelectrics*, **3**, 17–27.

HALL, S. R. & STEWART, J. M. (1990). Editors. *XTAL3.0 Users Manual*. Univs. of Western Australia, Australia, and Maryland, USA.

NEWNHAM, R. E., WOLFE, R. W., HORSEY, R. S., DIAZ-COLON, F. A. & KAY, M. I. (1973). *Mater. Res. Bull.* **8**, 1183–1195.

RAE, A. D. (1989). *RAELS89. A Comprehensive Constrined Least-Squares Refinement Program*. Univ. of New South Wales, Australia.

RAE, A. D., THOMPSON, J. G. & WITHERS, R. L. (1991). *Acta Cryst.* B**47**, 870–881.

RAE, A. D., THOMPSON, J. G., WITHERS, R. L. & WILLIS, A. C. (1990). *Acta Cryst.* B**46**, 474–487.

SHELDRICK, G. M. (1976). *SHELX76*. Program for crystal structure determination. Univ. of Cambridge, England.

SINGH, K., BOPARDIKAR, D. K. & ATKARE, D. V. (1988). *Ferroelectrics*, **82**, 55–67.

SUBBARAO, E. C. (1962). *J. Phys. Chem. Solids*, **23**, 665–676.

THOMPSON, J. G., RAE, A. D., WITHERS, R. L. & CRAIG, D. C. (1991). *Acta Cryst.* B**47**, 174–180.

WITHERS, R. L., THOMPSON, J. G. & RAE, A. D. (1991). *J. Solid State Chem.* **94**, 404–417.

WOLFE, R. W., NEWNHAM, R. E. & KAY, M. I. (1969). *Solid State Commun.* **7**, 1797–1801.

WOLFE, R. W., NEWNHAM, R. E., SMITH, T. K. & KAY, M. I. (1971). *Ferroelectrics*, **3**, 1–7.

Acta Cryst. (1992). B**48**, 428–437

Structure of $(\eta^6\text{-}C_6H_6)Mo(CO)_3$ at Room Temperature and 120 K: Motion about Equilibrium and Far from Equilibrium

BY HANS-BEAT BÜRGI AND ANDREA RASELLI

Laboratory for Chemical and Mineralogical Crystallography, University of Bern, CH-3012, Switzerland

AND DARIO BRAGA AND FABRIZIA GREPIONI

Dipartimento di Chimica 'G. Ciamician', Università di Bologna, Via F. Selmi 2, 40126 *Bologna, Italy*

(*Received* 28 *September* 1991; *accepted* 3 *December* 1991)

Abstract

The structure of (η^6-benzene)tricarbonylmolybdenum, $(\eta^6\text{-}C_6H_6)Mo(CO)_3$, has been determined at room temperature and 120 K by single-crystal X-ray diffractometry. The molecular motion about equilibrium has been studied by means of thermal-motion analysis, showing that there is significant stretching motion of C_6H_6 and CO relative to Mo. There are effects of molecular packing on the motion of the CO's and on the deviation of the molecular structure from C_{3v} symmetry which are mutually consistent. The motional features and the deviations from symmetry are very similar to those of the isostructural $(\eta^6\text{-}C_6H_6)Cr(CO)_3$. The reorientational motion of the C_6H_6 group has been explored by potential-energy-barrier calculations within the atom–atom approach. The results are compared with the available solid-state spectroscopic information. $(\eta^6\text{-}C_6H_6)Mo(CO)_3$ is monoclinic at room temperature [$a = 6.162$ (3), $b = 11.096$ (2), $c = 6.826$ (2) Å, $\beta = 101.64$ (3)°, $V = 457.12$ Å^3], and at 120 K [$a = 6.028$ (1), $b = 11.001$ (2), $c = 6.763$ (1) Å, $\beta = 100.79$ (1)°, $V = 440.55$ Å^3], space group $P2_1/m$, $Z = 2$.

Introduction

$(\eta^6\text{-}C_6H_6)M(CO)_3$ (M = Cr, Mo) represents the prototype of a large family of $(\eta^6$-arene$)ML_3$ species (Muetterties, Bleeke, Wucherer & Albright, 1982). The solid-state structure of $(\eta^6\text{-}C_6H_6)Cr(CO)_3$ has been studied at room and at low temperature by both X-ray and neutron diffraction methods (Corradini & Allegra, 1959; Bailey & Dahl, 1965*b*; Rees & Coppens, 1973; Wang, Angermund, Goddard & Kruger, 1987). The low-temperature structural work has shown that the C—C bonds '*trans*' to the chromium–carbonyl ones are shorter than the others by *ca* 0.017 Å (Rees & Coppens, 1973; Wang *et al.*, 1987). This result was also substantiated by extended Hückel calculations (Albright, Hofmann & Hoffman, 1977; Kok & Hall, 1985). We now report an X-ray crystallographic characterization of the Mo analogue at room temperature and 120 K. The aims of the paper can be summarized as follows:

0108-7681/92/040428-10$06.00

(i) To provide a brief comparative analysis of the structure of $(C_6H_6)Mo(CO)_3$ with that of (C_6H_6)-$Cr(CO)_3$ and of other known (η^6-arene)$M(CO)_3$ (M = Cr, Mo) species.

(ii) To study the small-amplitude motion of the entire molecule and some of its fragments by means of thermal-motion analysis (Dunitz, Schomaker & Trueblood, 1988; Bürgi, 1989) and to investigate the influence of crystal packing on such motion.

(iii) To investigate reorientational processes of the kind evidenced by various solid-state spectroscopic techniques for $(C_6H_6)Cr(CO)_3$ (Delise, Allegra, Mognaschi & Chierico, 1975; Chhor & Lucazeau, 1982; Lucazeau, Chhor, Sourisseau & Dianoux, 1983) and for $(C_6H_6)Mo(CO)_3$ (Lucazeau *et al.*, 1983). Potential-energy-barrier calculations based on the pairwise atom–atom approach (Pertsin & Kitaigorodsky, 1987) and thermal-motion analysis are combined for this purpose.

Experimental

All X-ray measurements were made on an Enraf–Nonius CAD-4 diffractometer equipped with a graphite monochromator (Mo $K\alpha$ radiation, λ = 0.71069 Å) and a Nonius low-temperature device. The intensities were collected in ω-scan mode at room temperature and at 120 K from the same crystal specimen, which had previously been enclosed in a glass capillary fixed with epoxy resin to the goniometer head. Unit-cell parameters were determined from 14 reflections with $15 < \theta < 20°$; four standard reflections (100, 043, 274, 575) were measured every 3600 s, with no significant change. Crystal data and details of measurements for the two data collections are summarized in Table 1. The chromium coordinates of $(C_6H_6)Cr(CO)_3$ at 78 K (Rees & Coppens, 1973) were used as the starting point for a difference Fourier synthesis and subsequent refinement of the $(C_6H_6)Mo(CO)_3$ low-temperature data. The resulting coordinates were used in turn as the starting point for refinement of the room-temperature data. Both analyses were based on real and imaginary scattering factors for neutral atoms taken from *International Tables for X-ray Crystallography* (1974, Vol. IV, pp. 99–149). For all calculations the *SHELX*76 program was used (Sheldrick, 1976).

Difference maps calculated from both full data sets showed weak peaks near expected H-atom positions. For the room-temperature analysis these positions were refined isotropically, while for the low-temperature analysis the same kind of refinement was carried out starting from calculated H-atom positions.

In the following RT and LT indicate the two structural determinations at room temperature and 120 K, respectively. The subscripts 'f' and 'h' are used to indicate the results of refinement with a full or high-order data set (Table 1). The following discussion will be confined mainly to a comparison between the results from the 'conventional' room-temperature full-data set, RT_f, and those from the low-temperature high-order refinement, LT_h. However, for reasons given below, we have chosen to report here (Table 2) fractional coordinates and anisotropic displacement parameters (a.d.p.'s) for RT_h and LT_h, while those for RT_f and LT_f are deposited as supplementary material.*

Table 1. *Crystal data and details of measurements for* $(C_6H_6)Mo(CO)_3$

	RT	120 K
Formula	$C_9H_6MoO_3$	$C_9H_6MoO_3$
M_r	258.08	258.08
Crystal size (mm)	0.15 × 0.10 × 0.08	0.15 × 0.10 × 0.08
System	Monoclinic	Monoclinic
Space group	$P2_1/m$	$P2_1/m$
a (Å)	6.162 (3)	6.028 (1)
b (Å)	11.096 (2)	11.001 (2)
c (Å)	6.826 (2)	6.763 (1)
β (°)	101.64 (3)	100.79 (1)
U (Å^3)	457.12	440.55
Z	2	2
$F(000)$	252	252
D_x (g cm^{-3})	1.87	1.95
λ(Mo $K\alpha$) (Å)	0.71069	0.71069
μ(Mo $K\alpha$) (cm^{-1})	13.69	14.20
θ range (°)	2–35	2–40
ω-scan width (°)	2.0	2.0
Requested counting $(I)/I$	0.03	0.03
Prescan rate (° min^{-1}), θ range (°)	16(20–35), 4(2–20)	2(35–40), 3(30–35), 4(20–30), 8(2–20)
Prescan acceptance $\sigma(I)/I$	1.0	1.0
Maximum scan time (s)	180	180
hkl range	−9, 9; 0, 17; 0, 10	−10, 10; 0, 19; 0, 12[a]
Measured reflections	2240	4235
Merging R	0.012,[b] 0.024[c]	0.017,[b] 0.025[c]
Min. and max. transmission for scan absorption correction (%)	95.55–99.97	95.6–100
Unique observed reflections $[F_o > 4\sigma(F_o)]$	1744,[b] 815[c]	2645,[b] 1677[c]
No. of refined parameters	78,[b] 64[c]	78,[b] 64[c]
R, R_G[d], S	0.022, 0.032, 2.529[b] 0.028, 0.026, 2.020[c]	0.019, 0.029, 3.797[b] 0.020, 0.021, 2.860[c]
k, g[d]	2.264, 0.00015[b] 2.644, 0.00000[c]	2.974, 0.0009[b] 2.860, 0.0002[c]
$(\Delta/\sigma)_{max}$	0.030[b] 0.001[c]	0.015[b] 0.008[c]
$(\Delta\rho)_{max}$, $(\Delta\rho)_{min}$ (e Å^{-3})	0.37, −0.34[b] 0.24, −0.18[c]	0.63, −0.74[b] 0.35, −0.40[c]

Notes: (*a*) Equivalent reflections −10, 0; 0, 19; −12, 0 were measured in the range $2 < \theta < 30°$. (*b*) Full data set. (*c*) High-order data: $0.63 < \sin\theta/\lambda < 0.82$ Å^{-1} (RT), $0.63 < \sin\theta/\lambda < 1.15$ Å^{-1} (120 K). (*d*) $R_G = [\sum(w(F_o - F_c)^2)/\sum(wF_o^2)]$, where $w = k/[\sigma^2(F) + g|F^2]$.

* Lists of atomic coordinates and anisotropic displacement parameters for RT_f and LT_f (Tables *S*I and *S*II), a full list of bond distances and angles (RT_f, *S*III; RT_h, *S*IV; LT_h, *S*V; LT_f, *S*VI), and observed and calculated structure factors (Tables *S*VII for RT and *S*VIII for LT) have been deposited with the British Library Document Supply Centre as Supplementary Publication No. SUP 54862 (32 pp.). Copies may be obtained through The Technical Editor, International Union of Crystallography, 5 Abbey Square, Chester CH1 2HU, England. [CIF reference: GE0298]

Table 2. *Fractional atomic coordinates and thermal parameters* ($Å^2$)

Thermal parameters are given in the form $\exp[-2\pi^2(U_{11}a^{*2}h^2 + \ldots + 2U_{12}a^*b^*hk + \ldots)]$. Coordinates and U's for the H atoms were fixed at the values obtained from full data set refinement.

	x	y	z	U_{iso} or U_{11}	U_{22}	U_{33}	U_{23}	U_{13}	U_{12}
RT_h									
Mo	0.33174 (4)	0.25	0.03310 (4)	0.0252 (2)	0.0318 (2)	0.0273 (2)	0.0000	0.0033 (1)	0.0000
C(1)	0.1903 (5)	0.1873 (3)	−0.3023 (4)	0.043 (1)	0.045 (1)	0.033 (1)	−0.005 (1)	0.002 (1)	−0.005 (1)
C(2)	0.3897 (8)	0.1232 (3)	−0.2315 (5)	0.063 (2)	0.041 (1)	0.042 (1)	−0.007 (1)	0.013 (1)	0.009 (1)
C(3)	0.5880 (5)	0.1858 (5)	−0.1602 (6)	0.038 (1)	0.078 (2)	0.048 (1)	0.001 (1)	0.013 (1)	0.016 (1)
C(4)	0.5611 (7)	0.25	0.2784 (7)	0.034 (1)	0.087 (4)	0.033 (1)	0.000	0.000	0.000
O(4)	0.7030 (11)	0.25	0.4153 (11)	0.048 (2)	0.181 (14)	0.043 (2)	0.000	−0.013 (2)	0.000
C(5)	0.1710 (6)	0.1301 (3)	0.1612 (5)	0.051 (1)	0.038 (1)	0.043 (1)	−0.003 (1)	0.016 (1)	−0.007 (1)
O(5)	0.0747 (15)	0.0610 (5)	0.2372 (10)	0.099 (4)	0.058 (2)	0.077 (3)	−0.001 (2)	0.042 (3)	−0.030 (2)
H(1)	0.057	0.139	−0.349	0.048					
H(2)	0.381	0.034	−0.229	0.047					
H(3)	0.712	0.134	−0.103	0.098					
LT_h									
Mo	0.33233 (2)	0.25	0.02771 (2)	0.0094 (1)	0.0106 (1)	0.0098 (1)	0.0000	0.006 (1)	0.0000
C(1)	0.19537 (17)	0.18628 (9)	−0.31053 (14)	0.0170 (3)	0.0155 (3)	0.0129 (3)	−0.0016 (2)	0.003 (2)	−0.0013 (2)
C(2)	0.3984 (2)	0.1213 (1)	−0.2377 (2)	0.0216 (4)	0.0152 (3)	0.0167 (3)	−0.0015 (3)	0.0034 (3)	0.0038 (3)
C(3)	0.5985 (2)	0.1854 (1)	−0.1662 (2)	0.0147 (3)	0.0267 (4)	0.0193 (4)	0.0001 (3)	0.0044 (3)	0.0051 (3)
C(4)	0.5633 (3)	0.25	0.2736 (2)	0.0147 (4)	0.0303 (7)	0.0128 (4)	0.0000	0.0002 (4)	0.0000
O(4)	0.7079 (3)	0.25	0.4133 (3)	0.019 (1)	0.068 (1)	0.016 (1)	0.000	−0.005 (1)	0.000
C(5)	0.1665 (2)	0.1296 (1)	0.1571 (2)	0.0195 (3)	0.0135 (3)	0.0162 (3)	−0.0003 (2)	0.0053 (2)	−0.0023 (3)
O(5)	0.0663 (3)	0.0593 (1)	0.2337 (2)	0.0373 (5)	0.0204 (4)	0.0282 (4)	0.0010 (3)	0.0143 (4)	−0.0101 (4)
H(1)	0.082	0.136	−0.343	0.015					
H(2)	0.394	0.042	−0.240	0.028					
H(3)	0.719	0.143	−0.130	0.026					

A comparison of relevant structural parameters obtained from the two kinds of data treatment at the two temperatures is given in Table 3. It can be seen that all bond distances between non-H atoms increase by between 0.007 and 0.026 Å on passing from RT_f to LT_h: mean M—C distances from 1.953 (2) to 1.960 (2) Å, and mean C≡O distances from 1.142 (2) to 1.162 (2) Å. This systematic and significant trend, especially in the C—O distances, is due to the differing contributions of the high-order data. Exclusion of the low-order data ($\sin\theta/\lambda < 0.63$ Å^{-1}) from the refinement of the low-temperature data (LT_h) reduces the error arising from the electron density deformation due to chemical bonding and lengthens the C≡O distances. This observation is confirmed by the results obtained with high-order refinement of the RT data (RT_h): 1.964 (4), 1.151 (8) Å, which are close to the results obtained for LT_h.

Structure of $(\eta^6\text{-}C_6H_6)Mo(CO)_3$

$(\eta^6\text{-}C_6H_6)Mo(CO)_3$ possesses a staggered conformation of the tricarbonyl group with respect to the ring atoms (see Fig. 1); a crystallographic mirror plane passes through the middle of two opposite C—C bonds and comprises one CO ligand. A comparison of structural parameters for $(\eta^6\text{-arene})M(CO)_3$ pairs (M = Cr, Mo) is presented in Table 4.

The Kekulè-type distortion of the benzene ring ascertained in $(C_6H_6)Cr(CO)_3$ by recent low-temperature X-ray and neutron diffraction studies (Rees & Coppens, 1973; Wang *et al.* 1987) is readily seen in both RT and LT determinations of $(C_6H_6)Mo(CO)_3$. The 'long' and 'short' bonds average 1.411 (4)'s and 1.389 (4), and 1.423 (2) and 1.403 (1) Å for RT_f and LT_h respectively [Δ = 0.022 (4) and 0.020 (2) Å], the difference being substantially equivalent to that reported for $(C_6H_6)Cr(CO)_3$ at 78 K [1.423 (2), 1.406 (2), Δ = 0.017 (2) Å].

M—C and C—O distances from different structure determinations are difficult to compare as it is known that these structural parameters are greatly affected by data-collection conditions and refinement strategy (Braga & Koetzle, 1987; Albano, Braga & Grepioni, 1989; De La Cruz & Sheppard, 1990). Nevertheless, the effect of substituting Mo for Cr deserves a closer look. It can be seen from Table 4 that the difference between Mo—C(arene) and Cr—C(arene) distances is invariably larger than that between the corresponding M—C(CO) ones. On average M—C(arene) distances increase by 0.154 Å, while M—C(CO) distances increase 0.125 Å on passing from Cr to Mo.

From Table 4 it is evident that the staggered conformation is generally preferred to the eclipsed one. On the other hand, the difference in energy between the two conformations is very small as shown by extended Hückel calculations (Albright *et al.* 1977; Kok & Hall, 1985) [1.3 kJ mol^{-1} in $(C_6H_6)Cr(CO)_3$] so that intermolecular forces can easily control the molecular structure in the solid state. $(C_6Et_6)M(CO)_3$ (M = Cr, Mo) (Iverson,

Table 3. *Comparison of the relevant bond distances* (Å) *and angles* (°) *from the room temperature* (*RT*) *and* 120 K (*LT*) *analyses for* (η^6-C_6H_6)Mo(CO)$_3$

	RT_f	RT_h	LT_f	LT_h
Sinθ/λ range (Å^{-1})	0.05–0.82	0.63–0.82	0.05–1.15	0.63–1.15
Mo—C(1)	2.378 (2)	2.383 (3)	2.385 (1)	2.387 (1)
Mo—C(2)	2.370 (2)	2.373 (4)	2.376 (1)	2.378 (1)
Mo—C(3)	2.356 (2)	2.363 (4)	2.364 (1)	2.364 (1)
Mo—C(4)	1.952 (3)	1.961 (4)	1.959 (1)	1.959 (1)
Mo—C(5)	1.953 (2)	1.966 (4)	1.961 (1)	1.961 (1)
C(4)—O(4)	1.135 (4)	1.143 (8)	1.152 (2)	1.159 (2)
C(5)—O(5)	1.146 (2)	1.155 (9)	1.158 (1)	1.162 (2)
Mo—C(4)—O(4)	177.1 (3)	177.4 (6)	176.7 (1)	176.7 (2)
Mo—C(5)—O(5)	179.2 (2)	179.0 (5)	179.3 (1)	179.2 (1)
C(1)—C(1′)	1.390 (4)	1.392 (7)	1.406 (2)	1.402 (2)
C(1)—C(2)	1.412 (3)	1.418 (5)	1.420 (2)	1.423 (1)
C(2)—C(3)	1.388 (4)	1.405 (6)	1.397 (2)	1.403 (2)
C(3)—C(3′)	1.410 (6)	1.426 (12)	1.431 (3)	1.422 (3)
C(1)—H(1)	0.99 (2)	0.98*	0.87 (1)	0.87*
C(2)—H(2)	1.00 (2)	0.99	0.87 (1)	0.88
C(3)—H(3)	0.99 (2)	0.98	0.86 (1)	0.86
C(1′)—C(1)—C(2)	120.1	120.1	120.1	120.2
C(1)—C(2)—C(3)	119.8 (2)	120.8 (3)	119.9 (1)	119.7 (1)
C(2)—C(3)—C(3)	120.1	119.6	120.1	120.2
C(1′)—C(1)—H(1)	123	123.1	129	129.2
C(2)—C(1)—H(1)	117 (2)	116.8	110.8 (5)	110.5
C(1)—C(2)—H(2)	117 (2)	117.6	118.4 (3)	118.5
C(3)—C(2)—H(2)	123 (2)	122.1	121.7 (3)	121.8
C(2)—C(3)—H(3)	113 (2)	113.7	117.2 (5)	116.6
C(3′)—C(3)—H(3)	126	126.4	123	123.1
C(4)—Mo—C(5)	87.7 (1)	87.8 (1)	87.8 (1)	87.8 (1)
C(5)—Mo—C(5′)	85.2 (1)	85.2 (2)	85.1 (1)	84.9 (1)

* H atoms were fixed at the positions obtained from the full data refinements.

Hunter, Blount, Damewood & Mislow, 1981) and ($C_6H_3Me_3$)Mo(CO)$_3$ (Koshland, Myers & Chesick, 1977; Iverson *et al.*, 1981) are eclipsed, probably because of dominant intramolecular forces.

Interestingly, the increase in *M*—C(CO) distances upon replacement of C_6H_6 in (C_6H_6)*M*(CO)$_3$ [giving *M*(CO)$_6$] is larger for *M* = Mo (0.099 Å) than for *M* = Cr (0.067 Å) (Whitaker & Jeffery, 1967; Mak, 1984). This may be taken as indicative of a stronger *trans* influence of the arenes on CO in Mo complexes than in Cr ones.

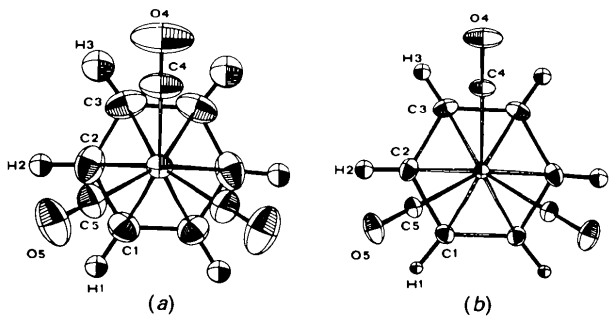

Fig. 1. *ORTEP* (Johnson, 1965) drawings of (η^6-C_6H_6)Mo(CO)$_3$, showing vibration ellipsoids at the 50% probability level: (*a*) RT; (*b*) 120 K.

Motion about equilibrium: thermal-motion analysis

In this section we analyse the atomic anisotropic displacement parameters. First we test the molecule or parts of it for non-rigidity using Hirshfeld's rigid-bond postulate (Hirshfeld, 1976). We find indications of intramolecular motion consistent with results from vibrational spectroscopy. Second, we apply the rigid-body model (Schomaker & Trueblood, 1968) to analyse observed displacement parameters **U**(obs). We are not primarily interested in the rigid-body motion parameters themselves, but rather in the differences **U**(obs) − **U**(rigid body) which – if significant – should provide additional indications of intramolecular motion.

In the subsequent analysis the graphic program *PEANUT* (Hummel, Hauser & Bürgi, 1990; Hummel, Raselli & Bürgi, 1990) is an important tool. It provides for several representations of anisotropic displacement parameters (a.d.p.'s). Apart from the usual equiprobability (thermal) ellipsoids, surfaces of mean-square or root-mean-square displacements may be plotted. They are based on $\langle u^2(\mathbf{n})\rangle = \mathbf{n}\mathbf{U}\mathbf{n}^T$ where $\mathbf{n}$ is a unit vector originating at the atomic position and pointing in an arbitrary direction, $\langle u^2(\mathbf{n})\rangle$ is the mean-square displacement in that direction. The surfaces defined by the endpoints of the vectors $|\langle u^2(\mathbf{n})\rangle|\mathbf{n}$ or $\langle u^2(\mathbf{n})\rangle^{1/2}\mathbf{n}$ are the mean-square or root-mean-square displacement surfaces respectively. The alternative representations are especially convenient for $\Delta\mathbf{U} = \mathbf{U}(\text{obs}) - \mathbf{U}(\text{rigid body})$ which may or may not be positive definite. If $\Delta\mathbf{U}$ is non-positive definite, the equiprobability surface is no longer a closed ellipsoid but an open hyperboloid. The set of vectors $|\langle \Delta u^2(\mathbf{n})\rangle|\mathbf{n}$ always defines a closed surface represented by solid lines if $\langle \Delta u^2(\mathbf{n})\rangle$ is positive and dotted lines if it is negative. Similarly, the vectors $\langle \Delta u^2(\mathbf{n})\rangle^{1/2}\mathbf{n}$ form a closed surface represented by solid lines if $\langle \Delta u^2(\mathbf{n})\rangle^{1/2}\mathbf{n}$ is positive and dotted lines if it is imaginary (see Fig. 2).

According to Hirshfeld's rigid-bond postulate, the difference between the mean-square displacement amplitudes (m.s.d.a.'s) of two covalently bonded atoms *A* and *B*, $\Delta_{A,B} = z^2_{A,B} - z^2_{B,A}$, evaluated along the bonding vector, should approach zero for atoms of comparable mass. The rigid-bond test may fail ($\Delta_{A,B} \neq 0$) when the displacement parameters are affected by inadequacies of the electron density model or of the diffraction data. It also fails, of course, when internal motion affects bonded atoms differently. We test for inadequacies of the model and the data first.

The $\Delta_{A,B}$ values for all atom pairs (excluding H atoms) from both full- and high-order RT and LT data sets are reported in Table 5. It can be seen that $|\Delta_{C,C}|$'s within the C_6 fragment are generally small, *i.e.* the fragment behaves essentially as a rigid body

Table 4. *Comparison of some relevant structural parameters for* $(\eta^6$-*arene*$)M(CO)_3$ *pairs* (M = Cr, Mo)

Mean bond lengths are given in Å (e.s.d.'s in parentheses).

		M—C(arene)	M—C(CO)	C—O	C—C(arene)	Conf.*	Ref.
$(C_6H_6)Mo(CO)_3$†	RT$_f$†	2.368 (2)	1.953 (2)	1.142 (4)	1.400 (4)	*S*	–
	RT$_h$	2.373 (4)	1.964 (4)	1.151 (8)	1.410 (8)		
	LT$_f$	2.375 (1)	1.960 (1)	1.156 (2)	1.415 (2)		
	LT$_h$	2.376 (1)	1.960 (1)	1.161 (2)	1.412 (2)		
$(C_6H_6)Cr(CO)_3$	RT	2.221 (8)	1.842 (9)	1.145 (7)	1.401 (10)	*S*	(1*a*)
	78 K	2.229 (2)	1.842 (2)	1.157 (2)	1.411 (2)		(1*b*)
Δ_{RT}/Δ_{LT}		0.147/0.147	0.111/0.118				
$(C_6H_5Me)Mo(CO)_3$		2.364 (2)	1.955 (2)	1.143 (3)	1.396 (5)	*S*	(2)
$(C_6H_5Me)Cr(CO)_3$		2.213 (5)	1.824 (4)	1.147 (6)	1.387 (7)	*E*	(3)
Δ		0.151	0.131				
$(C_6Me_6)Mo(CO)_3$		2.392 (4)	1.943 (4)	1.153 (5)	1.423 (6)	*S*	(4)
$(C_6Me_6)Cr(CO)_3$		2.233 (10)	1.814 (12)	1.163 (12)	1.417 (14)	*S*	(5)
Δ		0.169	0.129				
$(C_6Et_6)Mo(CO)_3$		2.384 (5)	1.946 (4)	1.165 (4)	1.425 (4)	*E*	(6)
$(C_6Et_6)Cr(CO)_3$		2.235 (3)	1.823 (3)	1.160 (4)	1.421 (3)	*E*	(6)
Δ		0.149	0.123				
$(C_6H_3Me_3)Mo(CO)_3$		2.371 (4)	1.964 (4)	1.153 (6)	1.408 (5)	*E*	(4)

References: (1*a*) Bailey & Dahl (1965*a*); (1*b*) Rees & Coppens (1973); (2) Braga & Grepioni (1990); (3) van Meurs & van Koningsveld (1977); (4) Koshland, Myers & Chesick (1977); (5) Bailey & Dahl (1965*b*); (6) Iverson, Hunter, Blount, Damewood & Mislow (1981).

* Conformation *S* = staggered, *E* = eclipsed.

† RT/LT results of room temperature and 120 K data collections, subscripts *f* and *h*: full data and high-order refinements, respectively.

at both temperatures. $\Delta_{O,C}$ values within the carbonyl groups are expected to be similarly small, since the triply bonded CO ligands constitute the most rigid fragment in the molecule. However, they are large and negative at room temperature when low-order data are included in the refinements; the differences almost disappear when only the high-order data are used. At low temperature, the values of $\Delta_{O,C}$ differ little between the two order refinements, presumably because the percentage of low-order data in the full data set is much smaller than at room temperature. This observation confirms previous observations that the a.d.p.'s of the C atoms (and to a lesser extent of the O atoms) of C≡O and C≡N ligands may be substantially affected by bonding electron density contributions (Hirshfeld, 1976; Braga & Koetzle, 1988). $\Delta_{Mo,C}$ values are consistently positive in all cases. The high-order refinements show that they tend to increase with increasing temperature.

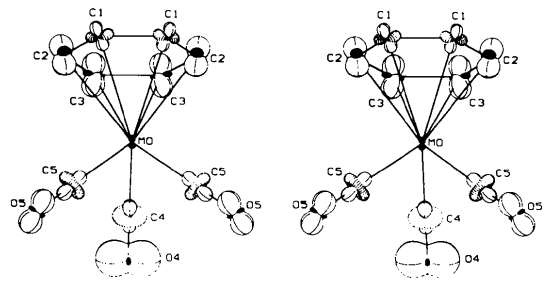

Fig. 2. Residual r.m.s. displacements $5 \times [U(obs) - U(model\ 1)]^{1/2}$: rigid-body motion of the entire molecule. Plain surfaces: positive residual motion; dotted surfaces: negative residual motion (Hummel, Hauser & Bürgi, 1990; Hummel, Raselli & Bürgi, 1990).

Overall, Δ's obtained from high-order refinement should thus seem to be more meaningful chemically. In order to test whether the Δ values from high-order refinement might be due to intramolecular motion, they may be compared to values calculated by normal coordinate analysis. The spectroscopic values, calculated on the basis of the normal coordinate analysis by Jones, McDowell & Goldblatt (1969), for $\Delta_{Mo,C(CO)}$ in $Mo(CO)_6$ are 0.0037 and 0.0023 Å^2 at 296 and 120 K, respectively. The average observed values of 0.0040 (9) and 0.0026 (3) Å^2 in $(\eta^6\text{-}C_6H_6)Mo(CO)_3$ are about of the same magnitude, as are the values for the Mo—C(benzene) bonds, 0.0030 (9) and 0.0026 (3) Å^2. Analogous quantities derived from a high-order refinement (Wang *et al.*, 1987) of the isostructural (C_6H_6)-$Cr(CO)_3$ are 0.0025 (4) Å^2 for Cr—C(CO) and 0.0024 (3) Å^2 for Cr—C(benzene) at 100 K. On the basis of the overall agreement between experiments and the spectroscopic results we conclude that the $\Delta_{M,C}$ values are not artefacts due to poor data or an insufficient model but reflect intramolecular motion of the ligands relative to the metal.

Although some Δ's show clear evidence for intramolecular motion, they represent only one aspect of such motion. The a.d.p.'s of the non-H atoms were

Table 5. *Differences between mean-square displacement amplitudes for* $(C_6H_6)Mo(CO)_3$

Values listed are 10^4 × m.s.d.a. for column atoms minus that for row atoms. The differences between symmetry equivalent atoms are zero.

RT_l [Range of $\sigma(\Delta U)$: 11–33]

	O(5)	C(5)	O(4)	C(4)	C(3)	C(3′)	C(2)	C(2′)	C(1)
Mo	23	77	44	68	20	20	16	16	12
C(1)	123	42	35	44	−7	−20	53	34	
C(2)	34	−14	55	26	36	29			
C(3)	−25	0	11	−48					
C(4)	−49	−34	−26						
O(4)	−115	−86							
C(5)	−54								

LT_l [Range of $\sigma(\Delta U)$: 3–8]

	O(5)	C(5)	O(4)	C(4)	C(3)	C(3′)	C(2)	C(2′)	C(1)
Mo	34	39	26	36	19	19	21	21	18
C(1)	57	19	14	10	−10	−7	1	−3	
C(2)	14	−14	26	−6	−8	1			
C(3)	13	1	18	−33					
C(4)	17	−6	−12						
O(4)	−14	−26							
C(5)	5								

RT_h [Range of $\sigma(\Delta U)$: 9–44*]

	O(5)	C(5)	O(4)	C(4)	C(3)	C(3′)	C(2)	C(2′)	C(1)
Mo	48	49	23	31	36	36	21	21	33
C(1)	119	26	11	5	−5	−4	41	8	
C(2)	−11	−66	50	9	−9	26			
C(3)	−13	−35	−3	−60					
C(4)	9	−22	−8						
O(4)	58	−73							
C(5)	−1								

LT_h [Range of $\sigma(\Delta U)$: 3–12]

	O(5)	C(5)	O(4)	C(4)	C(3)	C(3′)	C(2)	C(2′)	C(1)
Mo	22	23	15	29	28	28	30	30	21
C(1)	35	4	1	6	0	0	−1	−4	
C(2)	−4	−30	11	−8	2	4			
C(3)	−3	−17	−14	−36					
C(4)	6	−14	−14						
O(4)	−22	−30							
C(5)	0								

* Range of $\sigma(\Delta U)$ for all atom pairs not involving O(4). The range of $\sigma(\Delta U)$ for the atom pairs involving O(4) is 83–93.

Table 6. *Results of rigid-body-motion analysis for* $(C_6H_6)Mo(CO)_3$, *based on high-order refinements*

All vectors are referred to Cartesian axes along a, b, $a^* \times b^*$.

	296 K				120 K			
	Eigenvalue	Eigenvector			Eigenvalue	Eigenvector		
Model 1								
L_1 (deg^2)	42.98	−0.3465	0.0000	0.9380	16.09	−0.3703	0.0000	0.9289
L_2 (deg^2)	13.46	0.0000	−1.0000	0.0000	5.56	0.0000	−1.0000	0.0000
L_3 (deg^2)	11.08	0.9380	0.0000	0.3465	4.66	0.9289	0.0000	0.3703
T_1 (10^{-4}Å^2)	364	0.0000	−1.0000	0.0000	125	0.0000	−1.0000	0.0000
T_1 (10^{-4}Å^2)	302	0.6475	0.0000	−0.7621	116	0.7315	0.0000	−0.6819
T_1 (10^{-4}Å^2)	246	0.7621	0.0000	0.6475	90	0.6819	0.0000	0.7315
$\langle \Delta U^2 \rangle^{1/2}$ (Å^2)	10×10^{-4}				5×10^{-4}			
$\langle \sigma^2(U) \rangle^{1/2}$ (Å^2)	18×10^{-4}				9×10^{-4}			
GOF†	2.7				4.6			
Model 2								
L_1 (deg^2)	46.05	−0.1171	0.0000	0.9931	14.59	0.0819	0.0000	−0.9966
L_2 (deg^2)	17.74	0.9931	0.0000	0.1171	6.97	0.0000	1.0000	0.0000
L_3 (deg^2)	16.07	0.0000	1.0000	0.0000	6.81	0.9966	0.0000	0.0819
T_1 (10^{-4}Å^2)	303	0.0000	−1.0000	0.0000	111	0.6395	0.0000	−0.7688
T_1 (10^{-4}Å^2)	291	0.5208	0.0000	−0.8537	101	0.0000	1.0000	0.0000
T_1 (10^{-4}Å^2)	236	0.8537	0.0000	0.5208	84	0.7688	0.0000	0.6395
$\langle \Delta U^2 \rangle^{1/2}$ (Å^2)	4×10^{-4}				3×10^{-4}			
$\langle \sigma^2(U) \rangle^{1/2}$ (Å^2)	9×10^{-4}				6×10^{-4}			
GOF†	1.7				3.9			

†GOF = $\{\sum_N [w(U_{obs} - U_{calc})^2]/(N_{obs} - N_{var})\}^{1/2}$, where $w = 1/\sigma^2(U)$.

therefore also analyzed assuming a rigid-body model (Schomaker & Trueblood, 1968) either for the entire molecule (model 1) or for the more rigid $Mo(C_6H_6)$ fragment only (model 2, see Table 5). The program *THMA*11 (Trueblood, 1990) was used for this purpose. The eigenvalues of the **L** tensors for both models are indicative of a strongly anisotropic motion around the approximate molecular threefold symmetry axis (Table 6). Next we analyse the part of the a.d.p.'s not explained by the rigid-body models. Fig. 2 shows residual r.m.s. displacements for model 1. Three principal features are apparent: (1) Residual motion of benzene C atoms relative to Mo. The appearance of the residuals on C(1) differs from that of the residuals on C(2) and C(3). (2) Residual motion of the CO ligands in the direction of Mo. (3) O(4) shows substantial residual motion perpendicular to the molecular mirror plane, whereas the C atoms show negative residuals either in the benzene plane or perpendicular to the C≡O bonds [both features (1) and (2) are a pictorial representation of the Δ's discussed above]. Note that the overall pattern of residuals lacks the molecular C_{3v} symmetry. The positive and negative residuals are a consequence of the rigid-body least-squares fit to all atomic a.d.p.'s. Molecular libration about the approximate molecular threefold axis cannot accommodate the respective motions of C's and O's simul-

taneously. It does too much for C(4) and C(5) (negative residuals) and not enough for O(4). All these features confirm that the model of rigid-body motion is insufficient to account for the details of observed atomic motion, but they do not lead to obvious conclusions going significantly beyond those obtainable from inspection of the Δ's.

The situation is different for model 2, especially when placed in the context of molecular packing. The rigid-body motion parameters (**T**, **L**, **S**) (Schomaker & Trueblood, 1968) are obtained from a least-squares fit to, **U**(obs) of $Mo(C_6H_6)$ only (Table 6). Using these parameters, **U**(model) and differences **U**(obs) − **U**(model) have been calculated for all atoms including carbonyl groups. Again the differences show three principal features (Fig. 3): (1) The only motion left on C_6H_6 is that relative to Mo. It is very similar for all three C's and shows approximate C_{3v} symmetry. (2) There is significant motion of the CO's relative to Mo, as before. (3) There is a large positive residual on O(4) and a somewhat smaller one on C(4), both perpendicular to the mirror plane and a large negative one on O(5) and C(5) in the O(5)—Mo—O(5′) plane. The signs of the residuals on the CO's correlate with intermolecular contacts (Fig. 4). The closest neighbour of O(4) and C(4) in the direction of motion is H(2). Intermolecular distances are H(2)···C(4) 3.23 Å, ~ 3 Å after correction for the systematic shortening of C—H bonds in X-ray analyses, H(2)···O(4) 3.44 (~ 3.2) Å, angles are H(2)···C(4)···H(2) 167, H(2)···O(4)···H(2) 139°. In contrast, the closest neighbors of O(5) in the direction of the negative residuals are O(4) at a distance of 3.40 Å and H(3) at 2.73 (~ 2.5) Å, much shorter than the distance O(4)···H(2) discussed above. The angle O(4)···O(5)···H(3) is 164°, H(3)···O(5)···C(5) is 98° and the torsion angle H(3)···O(5)—Mo—O(5′) is ~ 180°, *i.e.* H(3) of the neighboring molecule is in the plane spanned by the two CO ligands in general position, the same plane that also contains the negative residuals on O(5) and C(5). Thus O(5) seems obstructed in its motion by the presence of H(3). This conclusion correlates nicely with the observation that the C(5)—Mo—C(5′) angle (84.9°) is ~ 3° smaller than C(5)—Mo—C(4) (87.8°).

One might ask which of the two models is preferable. We think model 2 is more informative for the following reasons: The motion of an *n*-atomic molecule in its crystalline environment may be thought of as being composed of six molecular translational and rotational oscillations (rigid-body part), of $3n-6$ internal motions and $3n(3n-1)/2$ contributions expressing the coupling between all of these. An analysis of atomic a.d.p.'s is equivalent to obtaining the best possible estimates for all contributions. The best possible estimate of the rigid-body motion is obtained from the most rigid part of the molecule (as judged from the Δ's). Here this is clearly the $Mo(C_6H_6)$ fragment rather than the entire molecule (Table 5). The goodness of fit at 296 and 120 K, respectively, is 1.7 and 3.9 for model 2 (excluding CO's), while it is poorer for model 1, *i.e.* higher at 2.7 and 4.6 (Table 6).

Model 2 disregards the molecular non-rigidity due to benzene rotation relative to $Mo(CO)_3$. This does

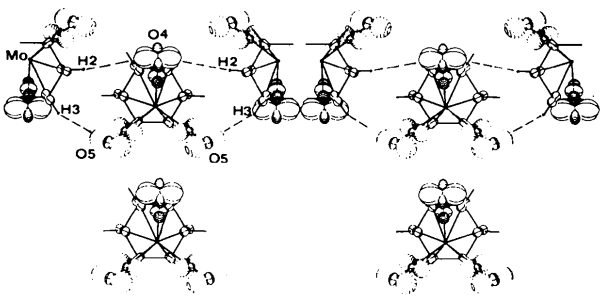

Fig. 4. Representation of residual r.m.s. displacements $5 \times$ [**U**(obs) − **U**(model 2)]$^{1/2}$ in relation to the closest neighboring fragments around the $(CO)_3$ group in $(C_6H_6)Mo(CO)_3$ (Hummel, Hauser & Bürgi, 1990; Hummel, Raselli & Bürgi, 1990). For the sake of clarity only the C—H bonds are drawn, the H atoms have the same number as the C atoms they are bonded to.

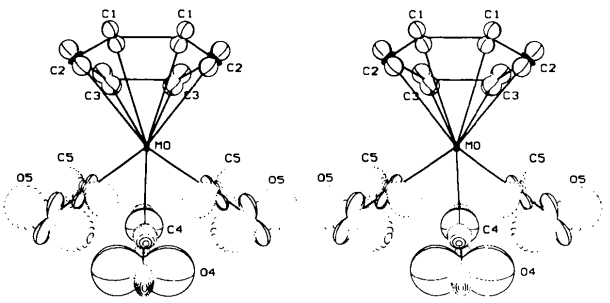

Fig. 3. Residual r.m.s. displacements $5 \times$ [**U**(obs) − **U**(model 2)]$^{1/2}$: rigid-body motion of the $Mo(C_6H_6)$ fragment only (Hummel, Hauser & Bürgi, 1990; Hummel, Raselli & Bürgi, 1990).

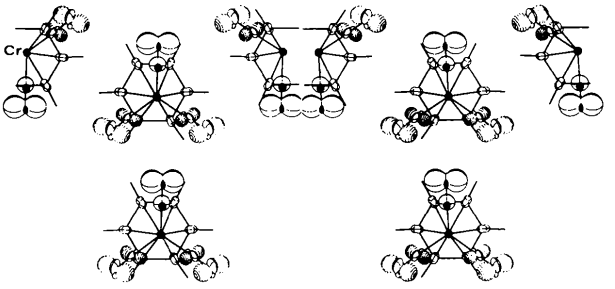

Fig. 5. Representation of residual r.m.s. displacements $5 \times$ [**U**(obs) − **U**(model 2)]$^{1/2}$ in relation to the closest neighboring fragments around the $(CO)_3$ group in $(C_6H_6)Cr(CO)_3$ (Hummel, Hauser & Bürgi, 1990; Hummel, Raselli & Bürgi, 1990). See caption to Fig. 4.

Table 7. *Comparison of the potential-energy barriers* (kJ mol^{-1}) *yielded by potential-energy calculations and spectroscopic techniques for* $(C_6H_6)Cr(CO)_3$ *and* $(C_6H_6)Mo(CO)_3$

ΔE values in parentheses are obtained without metal-atom contribution to the potential function. IQENS = incoherent quasi-elastic neutron scattering.

	ΔE	Raman (T) (Ref. 1)	IQENS (Ref. 2)	NMR
$(C_6H_6)Mo(CO)_3$ RT Benzene reorientation	24.7 (24.3)	-	-	16.7 (143–393 K) (Ref. 3)
$(C_6H_6)Mo(CO)_3$ 120 K Benzene reorientation	33.5 (33.1)	26.8 (120 K)		-
$(C_6H_6)Cr(Co)_3$ RT Benzene reorientation	19.7 (19.2)	19.7 (300 K)	15.5 (300 K)	17.6 (77-300 K) (Ref. 4)
$(C_6H_6)Cr(CO)_3$ 78 K Benzene reorientation	31.8 (31.4)	25.9 (120 K)	-	-

References: (1) Chhor & Lucazeau (1982); (2) Lucazeau *et al.* (1983); (3) S. Aime & R. Gobetto, personal communication; (4) Delise *et al.* (1975).

not change our conclusions, however. Suppose that due to internal benzene rotation the rigid-body part of rotation about the approximate molecular three-fold axis is actually smaller than suggested by model 2. This would imply that the negative residuals on O(5) and C(5) were less negative, and the positive residuals on O(4) and C(4) were even bigger, but the difference between them and its interpretation in terms of molecular packing would remain the same.

One might object that, in spite of the high-order refinements, the residuals in Fig. 4 are still largely due to inadequacies in the diffraction data and the model fitted to them. This appears unlikely after comparison of our results with those obtained for the isostructural $(C_6H_6)Cr(CO)_3$. A.d.p.'s obtained from a high-order refinement on very carefully measured diffraction data have been reported by Wang *et al.* (1987). Applying model 2 to these data leads to Fig. 5. Comparison with Fig. 4 shows that in essence the residual r.m.s. displacements are the same. It seems unlikely that the two independent measurements performed in different laboratories suffer from the same systematic deficiencies; we feel justified to conclude that the residuals represent motion characteristic of the two compounds.

In conclusion one might say that much more may be learned about the motion of molecules in crystals by scrupulously analysing accurate a.d.p.'s and comparing the results with molecular and packing geometry.

Motion far from equilibrium: potential-energy-barrier calculation

The reorientational motion of the benzene fragment in the solid state will now be evaluated. We have previously shown (Braga, Gradella & Grepioni, 1989; Braga & Grepioni, 1990, 1991; Braga, Grepioni, Johnson, Lewis & Martinelli, 1990; Aime, Braga, Gobetto, Grepioni & Orlandi, 1991) that the atom–atom pairwise potential-energy method (Kitaigorodsky, 1973; Gavezzotti & Simonetta, 1981, 1987) can be used to study the potential-energy changes associated with molecular fragment reorientational motions in solid neutral transition-metal complexes. Use is made of a Buckingham potential of the type p.p.e. $= \sum_i \sum_j [A\exp(-Br_{ij}) - Cr_{ij}^{-6}]$, where index i runs over all atoms of the reference molecule, and index j over the atoms of the surrounding molecules. The quantity r_{ij} represents the atom–atom intermolecular distance. The values of the coefficients A, B and C used in this work are those of Mirsky (1978, 1980). In keeping with this choice of potential parameters, the H-atom positions obtained by X-ray diffraction were replaced by calculated ones based on a C—H distance of 1.08 Å. For Cr and Mo potential parameters are not available; values for the corresponding noble gases (Kr and Xe) were used (Gavezzotti, 1982). The cutoff distance for summation is 10 Å; extension of this limit does not change the results. Ionic contributions are not considered. As a matter of fact atomic charges, determined in the case of $Cr(CO)_6$ from charge-density studies, are $q_C = 0.09\ (\pm 0.05)$ and $q_O = 0.12(\pm 0.05)$, *i.e.* very small (Rees & Mitschler, 1978). Packing potential energies (p.p.e.) were calculated by means of the computer program *OPEC* (Gavezzotti, 1983) for different conformations of the C_6H_6 fragment, which was rotated in steps of 10° about an axis passing through its center of mass and the Mo atom. The *relative* potential energy ΔE was calculated as ΔE = p.p.e. − p.p.e.(min) where p.p.e.(min) is the value corresponding to the observed structure (0° rotation). The results of the potential-energy calculations for both $(C_6H_6)Cr(CO)_3$ and $(C_6H_6)Mo(CO)_3$ are summarized in Table 7 and compared with the activation energy/potential barrier values available from spectroscopic experiments.

For benzene reorientation the potential-energy profiles, at the two temperatures, show minima of almost equal energy every 60°. The deviation of the benzene fragment from a regular hexagon, due to the bond-length alternation discussed above, is too small to cause an appreciable reduction of the angular periodicity to 120° in the potential-energy profile. No significant differences are observed if the metal-atom contributions are neglected.

The ΔE barrier to reorientation is calculated to be about 33.5 kJ mol^{-1} at 120 K while it decreases to about 25.1 kJ mol^{-1} at room temperature. Comparable values were obtained for $(C_6H_6)Cr(CO)_3$: ΔE = 31.4 at 78 K and 19.2 kJ mol^{-1} at room temperature (Braga & Grepioni, 1991). From Table 7 it can be seen that these potential barriers are systematically higher than the activation energies derived from spin-lattice proton-relaxation measurements (16.7 and 17.6 kJ mol^{-1} for M = Mo, and Cr, respectively). It should be kept in mind, however, that these latter values are obtained as mean values over broad temperature ranges. Since the experimental activation energies integrate several effects (such as correlated and uncorrelated jumping motion, relaxation of the environment, and *intramolecular* energy terms), which are not accounted for in ΔE(p.p.e.) calculations, one can only expect to obtain a calculated number that is of the same order of magnitude as the experimental one. In this context, it is important to stress that the similarity of the activation energies for benzene reorientation in the two complexes affords a good indication that the contribution to the total reorientational barrier arising from bonding interactions (during each 60° rotational jump, the benzene ring has to 'adjust' its geometry to the new situation) in $(C_6H_6)Mo(CO)_3$ can be expected to be of the same order of magnitude as in $(C_6H_6)Cr(CO)_3$ (1.3 kJ mol^{-1}), *i.e.* very small and negligible.

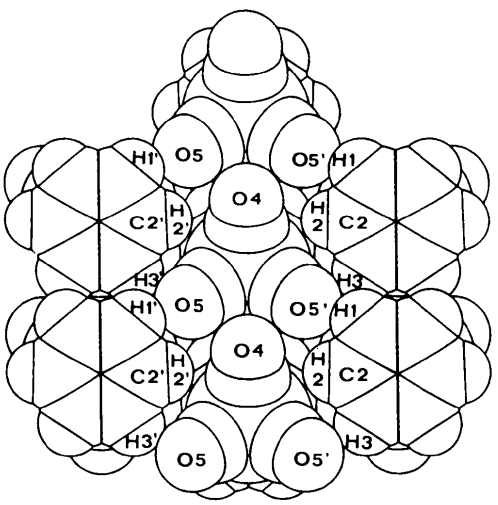

Fig. 6. Space-filling representation of the first six neighboring molecules determining the reorientational barrier of the tricarbonyl group in $(C_6H_6)Mo(CO)_3$.

An independent estimate of the potential-energy barriers at room temperature and 120 K can also be obtained using the method proposed by Dunitz & Maverick (1987). The estimate is based on the mean-square librational amplitudes of the benzene ring about its threefold axis ($\langle\varphi^2\rangle$ = 46.1 and 14.6 deg^2 at room temperature and 120 K, respectively). Quadratic approximation of a periodic cosine potential in the neighborhood of one of its minima leads to the expression $B = 2RT/n^2\langle\varphi^2\rangle$, where B is the barrier height and n the multiplicity of the barrier (here n = 6). The barrier heights thus obtained are 9.6 and 12.6 kJ mol^{-1}, at room temperature and 120 K, respectively. The quadratic approximation gives barriers that tend to be too low (Dunitz & Maverick, 1987). Indeed these estimates are somewhat lower than NMR values (see Table 6).

Reorientations of the molecule as a whole or of the tricarbonyl group in a static environment appear to be prevented by very high potential-energy barriers with maxima located at ± 60 and ± 180° from the minimum (ΔE > 350 kJ mol^{-1} at room temperature; ΔE > 600 kJ mol^{-1} at 120 K). The high barrier arises because of the efficient interlocking of the $(CO)_3$ groups in the lattice (see Fig. 6). As a matter of fact rotation of the tricarbonyl unit causes intermolecular 'clashes' between O(4) [O(5)] and atoms C(2) and H(2) [C(2′), H(2′)] (computed separation after + 60° rotation: 1.89, 1.37 Å, respectively) and between O(5′) and atoms O(4) and C(4) of the neighboring molecules (computed separation 1.90, 1.98 Å, respectively). The same behavior was observed for $(C_6H_6)Cr(CO)_3$. However, these barriers are much higher than those estimated from Raman frequencies, probably because the calculations do not allow for cooperative reorientations (Gavezzotti & Simonetta, 1976) of the neighboring molecules. The temperature dependence of the reorientational barriers implied in the computational model parallels that implied in the interpretation of the Raman frequencies (Chhor & Lucazeau, 1982), which is based on assumptions of the shape of the potential-energy surface.

With respect to Table 6 it can be concluded that the potential-energy barriers estimated within the 'static environment' approximation represent upper limits for the reorientational processes, whereas those estimated from the mean-square librational amplitude of the benzene ring provide a lower limit. In the case of benzene rotation the correct order of magnitude is predicted.

We wish to thank Dr P. Leoni and Professor M. Pasquali (Pisa) for preparing crystals of $(C_6H_6)Mo$-

$(CO)_3$. Financial support by Ministero dell'Università e della Ricerca Scientifica e Tecnologica and 'Schweizerischer Nationalfonds' is acknowledged.

References

AIME, S., BRAGA, D., GOBETTO, R., GREPIONI, F. & ORLANDI, A. (1991). *Inorg. Chem.* **30**, 951–956.

ALBANO, V. G., BRAGA, D. & GREPIONI, F. (1989). *Acta Cryst.* **B45**, 60–65.

ALBRIGHT, T. A., HOFMANN, P. & HOFFMAN, R. (1977). *J. Am. Chem. Soc.* **9**, 7546–7557.

BAILEY, M. F. & DAHL, L. F. (1965*a*). *Inorg. Chem.* **4**, 1298–1306.

BAILEY, M. F. & DAHL, L. F. (1965*b*). *Inorg. Chem.* **4**, 1314–1319.

BRAGA, D., GRADELLA, C. & GREPIONI, F. (1989). *J. Chem. Soc. Dalton Trans.* pp. 1721–1725.

BRAGA, D. & GREPIONI, F. (1990). *J. Chem. Soc. Dalton Trans.* pp. 3143–3146.

BRAGA, D. & GREPIONI, F. (1991). *Organometallics*, **10**, 2563–2569.

BRAGA, D., GREPIONI, F., JOHNSON, B. F. G., LEWIS, J. & MARTINELLI, M. (1990). *J. Chem. Soc. Dalton Trans.* pp. 1847–1852.

BRAGA, D. & KOETZLE, T. F. (1988). *Acta Cryst.* **B44**, 151–155.

BRAGA, D. & KOETZLE, T. F. (1987). *J. Chem. Soc. Chem. Commun.* pp. 144–146.

BRAGA, D. & KOETZLE, T. F. (1988). *Acta Cryst.* **B44**, 151–155.

BÜRGI, H.-B. (1989). *Acta Cryst.* **B45**, 383–390.

CHHOR, K. & LUCAZEAU, G. (1982). *J. Raman Spectrosc.* **13**, 235–246.

CORRADINI, P. & ALLEGRA, G. (1959). *J. Am. Chem. Soc.* **81**, 2271–2274.

DE LA CRUZ, C. & SHEPPARD, N. (1990). *J. Mol. Struct.* **224**, 141–161.

DELISE, P., ALLEGRA, G., MOGNASCHI, E. R. & CHIERICO, A. (1975). *J. Chem. Soc. Faraday Trans.* 2, **71**, 207–214.

DUNITZ, J. D. & MAVERICK, E. (1987). *Mol. Phys.* **62**, 451–459.

DUNITZ, J. D., SCHOMAKER, V. & TRUEBLOOD, K. N. (1988). *J. Phys. Chem.* **82**, 856–867.

GAVEZZOTTI, A. (1982). *Nouv. J. Chim.* **6**, 433–450.

GAVEZZOTTI, A. (1983). *J. Am. Chem. Soc.* **105**, 5220–5225.

GAVEZZOTTI, A. & SIMONETTA, M. (1976). *Acta Cryst.* A**32**, 997–1001.

GAVEZZOTTI, A. & SIMONETTA, M. (1981). *Chem. Rev.* **82**, 1–13.

GAVEZZOTTI, A. & SIMONETTA, M. (1987). In *Organic Solid State Chemistry*, edited by G. R. DESIRAJU. Amsterdam: Elsevier.

HIRSHFELD, F. L. (1976). *Acta Cryst.* A**32**, 239–244.

HUMMEL, W., HAUSER, J. & BÜRGI, H.-B. (1990). *J. Mol. Graphics*, **8**, 214–220.

HUMMEL, W., RASELLI, A. & BÜRGI, H.-B. (1990). *Acta Cryst.* B**46**, 683–692.

IVERSON, D. J., HUNTER, G., BLOUNT, J. F., DAMEWOOD, J. R. & MISLOW, K. (1981). *J. Am. Chem. Soc.* **103**, 6073–6083.

JOHNSON, C. K. (1965). *ORTEP*. Report ORNL-3794. Oak Ridge National Laboratory, Tennessee, USA.

JONES, L. H., MCDOWELL, R. S. & GOLDBLATT, M. (1969). *Inorg. Chem.* **8**, 2349–2353.

KITAIGORODSKY, A. I. (1973). *Molecular Crystals and Molecules*. New York: Academic Press.

KOK, R. A. & HALL, M. B. (1985). *J. Am. Chem. Soc.* **107**, 2599–2604.

KOSHLAND, D. E., MYERS, S. E. & CHESICK, J. P. (1977). *Acta Cryst.* **33**, 2013–2019.

LUCAZEAU, G., CHHOR, K., SOURISSEAU, C. & DIANOUX, A. (1983). *J. Chem. Phys.* **76**, 307–314.

MAK, T. C. W. (1984). *Z. Kristallogr.* **166**, 277–281.

MEURS, F. VAN & VAN KONINGSVELD, H. (1977). *J. Organomet. Chem.* **131**, 423–428.

MIRSKY, K. (1978). *Computing in Crystallography. Proceedings of the International Summer School on Crystallographic Computing*, pp. 169–182. Twente: Delft Univ. Press.

MIRSKY, K. (1980). *Chem. Phys.* **40**, 445–455.

MUETTERTIES, E. L., BLEEKE, J. R., WUCHERER, E. J. & ALBRIGHT, T. A. (1982). *Chem. Rev.* **82**, 499–525.

PERTSIN, A. J. & KITAIGORODSKY, A. I. (1987). *The Atom–Atom Potential Method*. Berlin: Springer-Verlag.

REES, B. & COPPENS, P. (1973). *Acta Cryst.* B**29**, 2515–2528.

REES, B. & MITSCHLER, A. (1978). *J. Am. Chem. Soc.* **98**, 7918–7924.

SCHOMAKER, V. & TRUEBLOOD, K. N. (1968). *Acta Cryst.* B**24**, 63–76.

SHELDRICK, G. M. (1976). *SHELX*76. Program for crystal structure determination. Univ. of Cambridge, England.

TRUEBLOOD, K. N. (1990). *THMA*11. Thermal motion analysis computer program. Univ. of California, Los Angeles, USA.

WANG, Y., ANGERMUND, K., GODDARD, R. & KRUGER, C. (1987). *J. Am. Chem. Soc.* **109**, 587–589.

WHITAKER, A. & JEFFERY, J. J. W. (1967). *Acta Cryst.* **23**, 977–989.